

1 The profound reach of the M8.6 11 April 2012
2 Indian Ocean earthquake: short-term global
3 triggering followed by a longer-term global shadow
4

5 April 3, 2013

6 Fred F. Pollitz¹, Roland Bürgmann², Ross S. Stein¹, and Volkan Sevilgen¹
7 ¹*USGS, Menlo Park, CA, USA* ²*Dept. Earth and Planetary Sci., UC*
8 *Berkeley, Berkeley CA*

9 **Abstract**

10 The M8.6 11 April 2012 Indian Ocean earthquake was an unusu-
11 ally large intra-oceanic strike-slip event. For several days the global
12 $M \geq 4.5$ and $M \geq 6.5$ seismicity rate at remote distances (i.e. thou-
13 sands of km from the mainshock) was elevated. But the $M \geq 6.5$ rate
14 subsequently dropped to zero for the succeeding 95 days, although the
15 $M \leq 6.0$ global rate was close to background during this period. Such
16 an extended period without a $M \geq 6.5$ event has happened rarely
17 over the past century, and never after a large mainshock. We inter-
18 pret both the short-lived global seismicity rate increase followed by the
19 longer-term quiescence as the products of dynamic stressing of a global

20 system of faults. Transient dynamic stresses can encourage short-term
21 triggering but paradoxically, can also inhibit rupture temporarily until
22 background tectonic loading restores the system to its pre-mainshock
23 stress levels. We construct a statistical model of global seismicity in-
24 volving tens of thousands of potential $M \geq 6.5$ source patches governed
25 by a single state variable (the shear strain) which is generally randomly
26 distributed among all possible strain states between fully relieved and
27 critically strained. When this system is subjected to a transient strain
28 of $\epsilon_d = 0.2 \mu\text{strain}$, approximately the transient perturbation of the
29 April 2012 event transmitted globally, we find that 6% of the patches
30 that were within ϵ_d of failure were triggered by passage of the seismic
31 waves; 88% of the remainder were inhibited from failure over the subse-
32 quent 100 days regardless of how close they were to failure before the
33 April 2012 mainshock. This carries important implications for fault
34 mechanics when faults are subjected to a transient stress.

35 **Introduction**

36 The M8.6 11 April 2012 earthquake was an exceptionally large strike-slip
37 event that occurred within oceanic lithosphere (McGuire and Beroza, 2012).
38 It was followed by an increase in global seismicity rates at magnitudes $4.5 \leq$
39 $M \leq 7.0$ for several days (Pollitz et al., 2012). A marked change in global
40 seismicity rates occurred over six-day periods pre- and post-mainshock, as
41 well as with respect to measures of background rates (Pollitz et al., 2012).
42 We depict it at $M \geq 6.5$ in Figure 1d, which indicates a briefly elevated rate
43 (0.4 events/day for 10 days) relative to three 100-day-long periods before
44 the event (averaging ~ 0.1 events/day).

45 Although other great earthquakes have triggered smaller earthquakes
46 and tremor worldwide, usually upon passage of the seismic waves (e.g. Pre-
47 jean et al., 2004; Velasco et al., 2008; Gonzales-Huizar et al., 2012), the
48 global seismicity response to the Indian Ocean event is unique because it
49 extends to large magnitudes (up to 7.0) and because it involves predomi-
50 nantly delayed triggered seismicity. This may be related to the high stress
51 drop and large Love-wave excitation associated with the event (McGuire
52 and Beroza, 2012; Meng et al., 2012; Yue et al., 2012), but much remains to
53 be explained, especially the mechanism of delayed triggering.

54 The April 2012 earthquake was remarkable in another aspect. The brief
55 acceleration in global seismic activity was followed by a nearly 100-day-long
56 quiescence at $M \geq 6.5$ (Figure 1e). We shall document that such a long
57 period without a large earthquake is rare. This raises the question as to its
58 association with the April 2012 mainshock, specifically whether the globally-
59 propagating seismic waves from the mainshock were capable of producing
60 not only a brief acceleration but also a longer-term quiescence.

61 A clue to the triggering power of the April 2012 event lies in the apparent
62 triggering of a foreshock sequence ~ 20 sec prior to a M3.9 dynamically-
63 triggered aftershock in Alaska (Tape et al., 2013). This suggests that source
64 patches that are close to failure may exhibit a gradual precursory slip prior
65 to generating a larger triggered event. This lends support to a model of
66 delayed dynamic triggering in which slow slip or small earthquakes cascades
67 into a larger triggered event (Peng and Gomberg, 2010; Shelly et al., 2011).
68 We consider a variation of this model in which source areas close to failure
69 are brought even closer to failure by propagating seismic waves, pushing

70 a substantial fraction of them over a stress threshold. In order to explain
71 the subsequent ~ 100 day shutdown in $M \geq 6.5$ activity, the model further
72 postulates a dynamic ‘shadow’ effect which can suppress seismicity even
73 when many source areas are close to failure and are expected to rupture.

74 In this study, we document both the post-mainshock short-term (10-
75 day) seismicity increase and the longer-term (subsequent 95-day) quies-
76 cence following the April 2012 Indian Ocean event. We then explore a
77 one-dimensional model of stressing of a global system of faults that pro-
78 duces $M \geq 6.5$ ruptures, forming a picture of the very different physics
79 which must underlie the observed post-mainshock global seismicity behav-
80 ior during these two time periods.

81 **Post-mainshock acceleration**

82 Figure 2 shows cumulative global $M \geq 4.5$ earthquake counts for a 4.2-year-
83 long period in an unedited catalog. Increases in cumulative $M \geq 4.5$ are
84 well correlated with the occurrence of $M \geq 6.5$ events (vertical dashed lines
85 and open circles in Figure 2, extended to $M \geq 6.4$). Increases are particu-
86 larly evident at the time of the M8.8 28 February 2010 Maule earthquake,
87 M9.0 11 March 2011 Tohoku earthquake, and M8.6 11 April 2012 Indian
88 Ocean earthquake. We also evaluate the same seismicity using a declustered
89 catalog designed to remove local aftershocks from the largest mainshocks.
90 The global catalog is edited such that all $M < 8.0$ events occurring within
91 one year following a $M \geq 8.0$ event and within 1500 km of it are excluded.
92 We refer to this as *large-mainshock declustering*. The resulting cumulative

93 global $M \geq 4.5$ earthquake counts and occurrence times of $M \geq 6.5$ events
94 are shown in Figure 3. The declustering has removed local aftershocks from
95 the Maule, Tohoku, and Indian Ocean events (and all other $M \geq 8.0$ main-
96 shocks). An increase at $M \geq 6.5$ following the Indian Ocean event, however,
97 is seen regardless of how the catalog is edited (e.g part (b) of these figures)
98 because these larger events are remote.

99 The $M \geq 5.5$ remote global seismicity was elevated at 99% significance
100 for the first two days following the event based on rate changes and absolute
101 rates derived from the first two days post-earthquake period (Pollitz et al.,
102 2012). The anomalous seismicity rates persist out to 10 days following the
103 mainshock at $M \geq 5.5$. This is based on comparing the observed seismicity
104 rate increase over the first 10 days with empirical probability distributions
105 derived from all 10-day periods following $M \geq 7$ mainshocks over the 20
106 years preceding the April 2012 event. Figure 4 reveals that the observed
107 seismicity rate exceeds the 95% tail of the empirical probability distributions
108 at magnitude thresholds of 5.5 and greater.

109 **Post-mainshock quiescence**

110 This initial acceleration in global earthquake rates (Figure 1d), including
111 seismicity at large magnitude up to M7.0, is unusual. Even more unusual is
112 the quiescence in $M \geq 6.5$ seismicity during the following 95 days – from 21
113 April to 26 July 2012 (Figure 1e). This pattern is remarkable when compared
114 with the three 100-day-long periods pre-mainshock and the subsequent 100-
115 day-long period post-mainshock (Figure 1a,b,c,f). The pattern is recast with

116 the 2008-2012 history of $M \geq 6.5$ events in Figures 2 and 3, which use no
117 catalog editing or large-mainshock declustering, respectively. The observed
118 95-day period is robust with respect to possible local aftershocks: it remains
119 even when global seismicity rates are evaluated without any catalog editing.

120 To address how often an extended globally quiet period has occurred, we
121 make use of the ISC-GEM catalog, which begins in 1900 and is intended to
122 supplant the Centennial Catalog (Engdahl and Villaseñor, 2002). The ISC-
123 GEM Global Instrumental Earthquake Catalogue (Storchak et al., 2012)
124 relocated 19,000 earthquakes during 1900-2009; it is the result of a special
125 effort to adapt and substantially extend and improve currently existing bul-
126 letin data. A million phase records were digitized, and all earthquakes were
127 relocated using Bondár and Storchak (2011). Approximate completeness is
128 $M \geq 7.50$ since 1900, $M \geq 6.25$ since 1918, and $M \geq 5.50$ since 1965.

129 Analysis of both the 30-year (1982-2012) NEIC catalog and the ISC-
130 GEM catalog shows that the background rate of remote $M \geq 6.5$ earth-
131 quakes is 0.105 events/day without editing and 0.089 events/day with large-
132 mainshock declustering. Using the latter value and assuming a Poissonian
133 distribution for event occurrence, this implies that the probability of realiz-
134 ing a 95-day interval with no $M \geq 6.5$ events is $\approx \exp[-8.45] = 2 \times 10^{-4}$.
135 The rarity of this is confirmed by compilation of $M \geq 6.5$ remote inter-event
136 times ΔT using the ISC-GEM catalog. To more accurately represent the
137 occurrence of remote $M \geq 6.5$ and reduce any possible bias towards low
138 ΔT in the historical catalog, we use large-mainshock declustering. Figure
139 5 shows that there are only three instances where inter-event periods were
140 longer than 95 days during the past century. The probability of realizing ΔT

141 longer than 95 days is 0.0012 for the past 95 years (Figure 5a) and 0.0011
142 for the past 59 years (Figure 5b).

143 The empirical probabilities for $\Delta T > 95$ days discussed above are based
144 on retrospective analysis using the observed interval of quiescence. Ret-
145rospective analysis can make an identified phenomenon appear significant
146 when in reality the phenomenon is bound to occur given a long enough
147 observation trial (e.g. Shearer and Stark, 2011). In the present case, the
148 fact that ΔT as long as 100 days has been observed a few times during
149 the past century indeed makes a single observation of such an interval not
150 necessarily significant. What is remarkable about the observation is that
151 it follows a very large seismic event by only several days. To put this in
152 perspective, we examine the pattern of $M \geq 6.5$ inter-event times in terms
153 of the elapsed time since the last large mainshock (i.e. that mainshock pre-
154ceding the first of two consecutive $M \geq 6.5$ events), which we restrict to
155 mainshocks of $M \geq 8.0$. This pattern is determined with large-mainshock
156 declustering, which tends to encourage longer ΔT in the historical catalog
157 and thereby make the post-Indian Ocean quiescent period less anomalous.
158 This pattern, shown in Figure 6, reveals that ΔT bears no systematic rela-
159tionship with elapsed time since a large event. This elapsed time since the
160 last large mainshock approximately follows a uniform distribution, and no
161 physical connection between the elapsed time and a long inter-event time is
162 warranted. Among the very large ($M \geq 8.5$) events, the April 2012 main-
163 shock stands apart because of its unusually long ΔT and short (10-day)
164 elapsed time since the mainshock.

165 **Magnitude-frequency statistics**

166 We wish to compare the April 2012 short-term increase and longer-term
167 decrease with background rates of ‘remote’ seismicity. Employing the NEIC
168 catalog and following Pollitz et al. (2012), this background is derived from
169 all 10-day intervals following $M \geq 7$ events during the four years preceding
170 the April 2012 Indian Ocean mainshock; the epicenter of each $M \geq 7$ event is
171 the center of an exclusion zone of radius 1500 km applied to each subsequent
172 10-day-long period. We do not extend the catalog further back in time in
173 order to ensure completeness at $M \geq 4.5$. Large-mainshock declustering
174 could be superimposed as an additional filter, but our prescription for the
175 background rates already removes the majority of local aftershocks (and it is
176 consistent with the measures defined below that we shall compare it with).
177 This background is shown with the filled circles in Figure 7.

178 Remote events during the 10 days following the April 2012 event are sim-
179 ilarly constrained to be > 1500 km from the 2012 Indian Ocean epicenter.
180 Their rates are shown with the triangles in Figure 7. Compared with back-
181 ground seismicity rates, the short-term (0-10 days post-mainshock) activity
182 at $M \geq 5.5$ is elevated.

183 We evaluate the global earthquake activity during the 10-105 days post-
184 Indian Ocean mainshock period and excluding those events < 1500 km from
185 the April 2012 epicenter. Their rates are shown with the open circles in Fig-
186 ure 7. At $M \geq 4.5$, the earthquake rates during the 10-105 days post-Indian
187 Ocean mainshock period are similar to the background in terms of their
188 magnitude-frequency statistics (Figure 7). The 10-105 days post-mainshock

189 period departs from background at $M > 6.0$ and lacks any $M \geq 6.4$ events.

190 **Statistical model of global seismicity**

191 **Conceptual model**

192 Pollitz et al. (2012) proposed that the globally-propagating seismic waves
193 generated by the Indian Ocean event stressed a sufficient number of close-
194 to-failure patches so that many of them were brought to failure in several
195 $M \gtrsim 5.5$ events within days of the mainshock. They likened the global
196 seismic response to the shaking of a tree full of apples, some of which were
197 ripe and inevitably shaken down by the seismic waves. Although this idea
198 was motivated by the very low seismicity rates in the 10 days prior to
199 11 April 2012, it serves as a useful conceptual model for how any set of
200 potentially-failing patches could be brought closer to failure by a transient
201 stress perturbation, i.e. propagating seismic waves. We envision that poten-
202 tial nucleation sites are in randomly distributed states between being relaxed
203 (presumably after their last significant rupture) and being critically stressed,
204 and that these sites age at a constant rate (assuming constant background
205 tectonic stressing). A consequence of these simple assumptions is that if
206 the reservoir of close-to-failure sites is perturbed by bringing a number of
207 those sites to failure within a short time (i.e., shortly after a dynamic stress
208 perturbation), then fewer sites will be available for failure in the subsequent
209 period.

210 To quantify this model, we suppose that there are N patches distributed
211 globally that may fail in a $M \geq 6.5$ event. On these patches we assume an

212 average strain accumulation rate $\dot{\epsilon}$, strain release $\Delta\epsilon$, and average combined
 213 rate of rupture λ . Let $\{\epsilon_i, i = 1, \dots, N\}$ be the patch strains. From their
 214 rate of combined rupture, these strains are randomly distributed such that
 215 within a time interval Δt , the probability of a rupture on the collection of
 216 patches is

$$\prod_{i=1}^N \text{P}[\epsilon_i - \epsilon_{\text{crit}} < -\dot{\epsilon}\Delta t] = e^{-\lambda\Delta t} \quad (1)$$

217 where ϵ_{crit} ($> \epsilon_i$ for all i) is a critical strain threshold such that rupture on
 218 a given patch will occur when strain builds up to that value. Assuming the
 219 $\{\epsilon_i\}$ are identically distributed, for one patch we have

$$\text{P}[\epsilon_i - \epsilon_{\text{crit}} < -\dot{\epsilon}\Delta t] = e^{-\lambda\Delta t/N} \quad (2)$$

220 **Short-term triggering**

221 We hypothesize that transient strains from the April 2012 event led to short-
 222 term rupture of a fraction f_1 of available patches that were within ϵ_d of
 223 failure; these would correspond to the four $M \geq 6.5$ events which actually
 224 occurred during the first 10 postseismic days (Figure 1d; Figure 3b). We
 225 choose $\epsilon_d = 0.1 \mu\text{strain}$ based on the order of magnitude of the amplitude
 226 of transient strains transmitted globally (Pollitz et al., 2012). Define L to
 227 be the number of $M \geq 6.5$ patches expected to be within ϵ_d of failure upon
 228 the occurrence of the April 2012 event, so that the number of patches which
 229 ruptured in the short-term is Lf_1 . If strain states are randomly distributed

230 between $\epsilon_{\text{crit}} - \Delta\epsilon$ and ϵ_{crit} , then

$$L = N \frac{\epsilon_{\text{d}}}{\Delta\epsilon} \quad (3)$$

231 Eqn 3 is consistent with the empirical result that the number of far-field
232 triggered events tends to scale linearly with the amplitude of the peak dy-
233 namic strain (van der Elst and Brodsky, 2010). Since patches undergo a
234 strain drop $\Delta\epsilon$ when they fail, the left-hand-side of eqn 2 is $\exp(-\dot{\epsilon}\Delta t/\Delta\epsilon)$.
235 Equating this with the right-hand-side of eqn 2 yields

$$N = \lambda \frac{\Delta\epsilon}{\dot{\epsilon}} \quad (4)$$

236 which, combined with eqn 3 yields

$$L = \lambda \frac{\epsilon_{\text{d}}}{\dot{\epsilon}} \quad (5)$$

237 **Longer-term quiescence**

238 The global system yields Lf_1 short-term triggered events. These events
239 are by themselves insufficient to account for the budget of expected $M \geq$
240 6.5 events within 105 days following the Indian Ocean mainshock. This is
241 illustrated in Figure 8, which shows the cumulative number of $M \geq 6.5$
242 events using the NEIC catalog with large-mainshock declustering. The solid
243 gray line with slope 0.089 events/day represents the 30-year background
244 rate. When this rate is extrapolated to 105 days post-mainshock, 9.4 $M \geq$
245 6.5 events should have occurred during this time; only four occurred (i.e.

246 those of the first 10 days), leaving an apparent gap of 5.4 events. If this
 247 arithmetic were correct, then the quiescence is roughly twice as long as
 248 would be expected for the number of short-term (triggered) $M \geq 6.5$ events.
 249 However, if these four events were considered as a separate phenomenon, i.e.
 250 dynamically triggered events, not part of the budget of expected $M \geq 6.5$
 251 events, then there would be an even larger gap in the number of $M \geq 6.5$
 252 events expected to occur over the succeeding 95 days (i.e. from 10 to 105
 253 days post-mainshock) – 8.4 events as indicated Figure 8.

254 As we are dealing with the statistics of small numbers, any observed
 255 gap may be a random, albeit rare, statistical fluctuation with no physical
 256 underpinnings. The alternative would be to propose that after the April
 257 2012 mainshock, a fraction f_2 of the remaining $L \times (1 - f_1)$ close-to-failure
 258 patches were made ‘ineligible’ for rupture, notwithstanding their strain state,
 259 by some process associated with dynamic stressing from the mainshock.
 260 We may interpret the $T_{\text{quiet}} = 95$ day interval without $M \geq 6.5$ events
 261 as the amount of time that the reset system needed to have a probability
 262 $1 - \exp(-1)$ of producing an event. Specifically,

$$\prod_{i=1}^{L(1-f_1)(1-f_2)} \text{P} [\epsilon_i - \epsilon_{\text{crit}} < -\dot{\epsilon}T_{\text{quiet}}] = e^{-1} \quad (6)$$

263 Note that eqn 6 accounts for the occurrence of the Lf_1 events during the
 264 initial short-term activity. Assuming that these eligible $L(1 - f_1)(1 - f_2)$
 265 close-to-failure patches are identically distributed, for one patch we have

$$\text{P} [\epsilon_i - \epsilon_{\text{crit}} < -\dot{\epsilon}T_{\text{quiet}}] = e^{-1/[L(1-f_1)(1-f_2)]} \quad (7)$$

266 If these ϵ_i are uniformly distributed over the interval $(\epsilon_{\text{crit}} - \epsilon_{\text{d}}, \epsilon_{\text{crit}})$, then
 267 the left-hand-side of eqn 7 is $\exp[-\dot{\epsilon}T_{\text{quiet}}/\epsilon_{\text{d}}]$. Equating this with the right-
 268 hand-side of eqn 7 yields

$$L(1 - f_1)(1 - f_2) = \frac{1}{T_{\text{quiet}}} \frac{\epsilon_{\text{d}}}{\dot{\epsilon}} \quad (8)$$

269 Substituting eqn 5 for L into eqn 8 yields

$$f_2 = 1 - \frac{1}{1 - f_1} \frac{1}{\lambda T_{\text{quiet}}} \quad (9)$$

270 Combining eqns 5 and 9 with the constraint $Lf_1 = 4$ (the number of
 271 short-term triggered events, i.e. Figures 1d and 3b, we may solve for L , f_1 ,
 272 and f_2 . Using parameter values $\dot{\epsilon} = 0.05 \mu\text{strain}/\text{yr}$ and $\epsilon_{\text{d}} = 0.1 \mu\text{strain}$,
 273 this yields $L = 66$, $f_1 = 0.061$ and $f_2 = 0.88$. The estimate of L is sensible,
 274 as it represents the number of patches that are within $0.1 \mu\text{strain}$ of failure
 275 with a loading rate of $0.05 \mu\text{strain}/\text{yr}$, i.e. the number of nucleation sites
 276 that ripen in a two-year time interval. We expect $66 M \geq 6.5$ events to
 277 occur within an average two-year timespan given the occurrence rate of
 278 $\lambda = 0.089/\text{day}$.

279 Discussion

280 The total number of $M \geq 6.5$ source patches N is given by eqn 4 for
 281 a suitable choice of $\Delta\epsilon$. A typical stress drop of 3 MPa corresponds to
 282 $\Delta\epsilon = 50 \mu\text{strain}$, leading to $N = 32,800$ total source patches. The fault
 283 area corresponding to $M = 6.5$ is 164 km^2 (Wells and Coppersmith, 1994),

284 so the minimum area of our idealized system is $5.4 \times 10^6 \text{ km}^2$ (minimum
285 because fault area is larger for $M > 6.5$). This is comparable with the to-
286 tal area along the seismogenic portion of the worlds’s subduction zones and
287 transform faults. A total length of the global subduction zones of 43,500
288 km (von Huene and Scholl, 2012) times 150 km downdip distance yields
289 $6.5 \times 10^6 \text{ km}^2$. A total length of transform faults of 44,433 km (Bird et al.,
290 2002) times a mean ‘coupled lithosphere thickness’ of 3 km (Bird et al., 2002)
291 yields $0.1 \times 10^6 \text{ km}^2$, for a total of $6.6 \times 10^6 \text{ km}^2$. The fault area calculated
292 from our simple statistical model is approximately the area of active faults
293 that were subject to high transient strain.

294 Eqn 9 states that the fraction f_2 of inhibited patches is larger when the
295 product λT_{quiet} is larger. The latter is simply the 8.4-quake gap illustrated in
296 Figure 8. The equation also states that $1 - f_2$ is inversely proportional to $1 -$
297 f_1 , so if a larger fraction of available ‘ripe’ nucleation patches had ruptured in
298 the short term, f_1 would be larger and f_2 would be correspondingly smaller.
299 Since inferred f_1 is small, the four events which occurred in the short term
300 are only a small fraction of the nucleation sites that were probably close
301 to failure. In other words, the occurrence of these four events removed an
302 insignificant number of sites from the pool of close-to-failure sites.

303 The fraction of inhibited ruptures would be smaller if the number of
304 close-to-failure sites L were smaller than prescribed by eqn 5, as would be
305 the case if $M \geq 6.5$ -quake productivity were unusually high for a long period
306 before the 11 April 2012 event. However, the pre-mainshock productivity
307 appears no different from the 30-year background level (Figure 8). The
308 fraction of inhibited ruptures would also be smaller if it were supposed that

309 the short-term triggered events represented those patches closest to rupture
310 at the time of the 11 April 2012 mainshock, i.e. those ‘next in line’ to
311 rupture had the 11 April 2012 event not occurred. In that case, our analysis
312 would still require a fraction $f_2 = 1 - 1/(5.4 \text{ events}) = 81\%$ to have been
313 inhibited from rupture, consistent with the 5.4-event gap depicted in Figure
314 8. We conclude that regardless of its effective size, the 5 to 9-quake gap
315 accumulated over the 105-day period following the 11 April 2012 mainshock
316 is either statistically uncertain, or needs to be accounted for by inhibiting
317 rupture of nucleation sites that would have been expected to ripen during
318 this time.

319 If the quiescence following the April 2012 earthquake is indeed larger
320 than expected to catch up to the long term $M \geq 6.5$ rate after the short-
321 term burst, then this calls into question the notion that dynamic stresses
322 can only increase earthquake rates rather than inhibit them. This has been
323 used as the basis for discriminating between the mechanisms of dynamic
324 stressing and the static stress change (e.g. Gomberg et al., 1998; Felzer and
325 Brodsky, 2005; Toda et al., 2012). Our results for one M8.6 mainshock
326 suggest that dynamic stresses lead to increased global seismicity rates in the
327 ‘short term’ (everywhere that dynamic stresses are sufficiently high) and
328 are thus consistent with this assumption. The idea that a dynamic ‘stress
329 shadow’ can develop over a longer time scale is suggested by our results but
330 needs to be confirmed by additional studies at regional scales. This could be
331 done by repeating the analysis of Parsons and Velasco (2011) at intermediate
332 distances from the largest ($M \geq 8$) earthquakes in their dataset, or by re-
333 visiting cases where clear short-term increases are explicable with dynamic

334 stressing (e.g. Kilb et al., 2000; Gomberg et al., 2003; Brodsky and Prejean,
335 2005; Hill and Prejean, 2007).

336 **Implications for earthquake physics**

337 Our results suggest that roughly 6% of those patches that would have been
338 temporarily strained above ϵ_{crit} by the seismic waves did actually rupture.
339 Of those that did not rupture, roughly 88% were somehow removed from
340 the eligible pool of potentially-failing sites on a 100-day timescale, regard-
341 less of the fact that they had been previously close to failure. This removal
342 of apparently close-to-failure sites from being capable of rupturing at the
343 $M \geq 6.5$ level is surprising, and might have two possible explanations:

344 (1) Transient mainshock stresses may have changed the state of close-to-
345 failure patches, delaying an ongoing process of cascade to failure.

346 (2) Dynamic changes in permeability could reduce the effective stress along
347 a fault, e.g. by changing the distribution of pore fluid pressures and hence
348 effective coefficient of friction along the patch.

349

350 The first explanation, involving changing the state of a fault by dynamic
351 stresses e.g. through an increase in the mean critical slip distance D_c , has
352 been previously proposed by Parsons (2005) as a mechanism for delayed
353 triggering. We suggest that it is a possible mechanism for delaying a rup-
354 ture even if it was impending in the absence of transient dynamic stresses.
355 In the context of rate-and-state friction theory, Parsons (2005) notes that
356 while seismically-induced reductions in D_c may occur (and lead to increased

357 seismicity rates), it is also physically plausible that dynamic stresses could
358 increase D_c (and lead to reduced seismicity rates).

359 The second explanation is based on the fact that faults tend to have
360 a low-permeability core surrounded by a high-permeability damage zone
361 (Caine et al., 1996), and transient stresses may suddenly reduce permeability
362 on a fault, temporarily allowing local pore pressure changes that may trigger
363 earthquakes (e.g. Brodsky et al., 2003). The recovery process after an initial
364 perturbation, however, will act to reduce fault zone permeability (section 4
365 of Manga et al. (2012)). Although the recovery process is thought to return
366 the fault zone to its pre-existing state, it is conceivable that a fault zone may
367 undergo a net decrease in effective stress, possibly by expulsion of fluids from
368 the fault zone during the initial perturbation.

369 **Conclusions**

370 The M8.6 11 April 2011 earthquake is a unique seismic event in terms of the
371 ensuing global seismic activity, characterized by a brief acceleration followed
372 by a very long shutdown in $M \geq 6.5$ seismicity. We believe that these two
373 characteristics are related and are the product of dynamic stressing from the
374 mainshock. Using a one-dimensional model of stressing of the global system
375 of faults subject to a simple failure criterion, we find that: (1) a small
376 fraction of the reservoir of available close-to-failure patches were brought
377 to failure, leading to the short-term seismicity rate increase, and (2) most
378 other patches that might have been brought to failure during the subsequent
379 95 days were made temporarily incapable of sustaining a $M \geq 6.5$ rupture.

380 The first finding is a consequence of the transient stressing of close-to-failure
381 patches temporarily above their failure threshold. The second finding is
382 surprising and, if true, would imply that transient dynamic stressing from
383 a large distant event can change the state of a fault such as to temporarily
384 inhibit a large rupture.

385 **Data and Resources**

386 Seismic hypocenters and magnitudes were provided by the National Earth-
387 quake Information Center (NEIC) catalog and the ISC-GEM catalog. The
388 ISC-GEM catalog is a component of the Global Earthquake Model effort
389 (<http://www.globearthquakemodel.org>, last accessed March 2013).

390 **Acknowledgements**

391 We thank Jeanne Hardebeck and Ruth Harris for their internal reviews of a
392 preliminary draft.

393 **References**

- 394 Bird, P., Kagan, Y., and Jackson, D. (2002). Plate Tectonics and Earth-
395 quake Potential of Spreading Ridges and Oceanic Transform Faults. In
396 Stein, S. and Freymueller, J., editors, *Plate Boundary Zones*, number 30,
397 pages 203–218. American Geophysical Union, Washington, DC.
- 398 Bondár, I. and Storchak, D. (2011). Improved location procedures at the
399 international seismological centre. *Geophys. J. Int.*, 186:1220–1244.

- 400 Brodsky, E. E. and Prejean, S. G. (2005). New constraints on mechanisms
401 of remotely triggered seismicity at Long Valley Caldera. *J. Geophys. Res.*,
402 110:B04302,doi:10.1029/2004JB003211.
- 403 Brodsky, E. E., Roeloffs, E., Woodcock, D., Gall, I., and Manga, M. (2003).
404 A mechanism for sustained groundwater pressure changes induced by dis-
405 tant earthquakes. *J. Geophys. Res.*, 108:2390,doi:10.1029/2002JB002321.
- 406 Caine, J. S., Evans, J. P., and Forster, C. B. (1996). Fault zone architecture
407 and permeability structure. *Geology*, 24:1025–1028.
- 408 Engdahl, E. E. and Villaseñor, A. (2002). Global Seismicity: 1900-1999.
409 In Lee, W. H. K., editor, *International Handbook of Earthquake and*
410 *Engineering Seismology*, pages doi:10.1016/S0074–6142(02)80244–3. Aca-
411 demic, Amsterdam.
- 412 Felzer, K. R. and Brodsky, E. E. (2005). Testing the stress shadow hypoth-
413 esis. *J. Geophys. Res.*, 110:doi:10.1029/2004JB003277.
- 414 Gomberg, J., Blanpied, M. L., and Beeler, N. M. (1998). Earthquake trig-
415 gering by transient and static deformation. *J. Geophys. Res.*, 103:24,411–
416 24,426.
- 417 Gomberg, J., Bodin, P., and Reasenber, P. A. (2003). Observing earth-
418 quakes triggered in the near field by dynamic deformations,. *Bull. Seismol.*
419 *Soc. Am.*, 93:118–138.
- 420 Gonzales-Huizar, H., Velasco, A. A., Peng, Z., and Castro, R. R. (2012).

421 Remote triggered seismicity caused by the 2011 M9.0 Tohoku-Oki, Japan
422 earthquake. *Geophys. Res. Lett.*, 39:L10302, doi:10.1029/2012GL051015.

423 Hill, D. P. and Prejean, S. (2007). Dynamic triggering. In Schubert, G.,
424 editor, *Treatise on Geophysics*, volume 4 Earthquake Seismology, pages
425 258–288. Elsevier.

426 Kilb, D., Gomberg, J., and Bodin, P. (2000). Triggering of earthquake
427 aftershocks by dynamic stresses. *Nature*, 408:570–574.

428 Manga, M., Beresnev, I., Brodsky, E. E., Elkhury, J. E., Elsworth, D.,
429 Ingebritsen, S. E., Mays, D. C., and Wang, C.-Y. (2012). Changes in per-
430 meability caused by transient stresses: Field observations, experiments,
431 and mechanisms. *Rev. Geophys.*, 50:8755–1209/12/2011RG000382.

432 McGuire, J. and Beroza, G. (2012). A Rogue Earthquake Off Sumatra.
433 *Science Express*, page 10.1126/science.1223983.

434 Meng, L., Ampuero, J.-P., Stock, J., Duputel, Z., Luo, Y., and Tsai,
435 V. C. (2012). Earthquake in a maze: compressional rupture branch-
436 ing during the 2012 Mw 8.6 Sumatra earthquake. *Science*, 337:724–726,
437 doi:10.1126/science.1224030.

438 Parsons, T. (2005). A hypothesis for delayed dynamic earthquake triggering.
439 *Geophys. Res. Lett.*, 32:L04302, doi:10.1029/2004GL021811.

440 Parsons, T. and Velasco, A. A. (2011). Absence of remotely triggered large
441 earthquakes beyond the mainshock region. *Nature Geoscience*, 4:312–316.

442 Peng, Z. and Gomberg, J. (2010). An integrated perspective of the contin-
443 uum between earthquakes and slow-slip phenomena. *Nature Geoscience*,
444 3:599–607.

445 Pollitz, F., Stein, R. S., Sevilgen, V., and Bürgmann, R. (2012). The 11 April
446 2012 east Indian Ocean earthquake triggered large aftershocks worldwide.
447 *Nature*, 490:250–253.

448 Prejean, K., Hill, D. P., Brodsky, E. E., Hough, S. E., Johnston, M. J. S.,
449 Malone, S. D., Oppenheimer, D. H., Pitt, A. M., and Richards-Dinger,
450 K. B. (2004). Remotely triggered seismicity on the United States west
451 coast following the M_w 7.9 Denali Fault earthquake. *Bull. Seism. Soc.*
452 *Am.*, 94:S348–S359.

453 Shearer, P. and Stark, P. (2011). Global risk of big earthquakes has not
454 recently increased. *PNAS*, 109:717–721.

455 Shelly, D. R., Peng, Z., Hill, D. P., and Aiken, C. (2011). Triggered creep
456 as a possible mechanism for delayed dynamic triggering of tremor and
457 earthquakes. *Nature Geoscience*, 4:384–388.

458 Storchak, D. A., Di Giacomo, D., Bondár, I., and Harris, J. (2012). The ISC-
459 GEM Global Instrumental Reference Earthquake Catalogue (1900-2009).
460 *AGU Fall Meeting, San Francisco, CA*.

461 Tape, C., West, M., Silwal, V., and Ruppert, N. (2013). Earthquake nu-
462 cleation and triggering on an optimally oriented fault. *Earth Planet. Sci.*
463 *Lett.*, in press.

464 Toda, S., Stein, R. S., Beroza, G. C., and Marsan, D. (2012).
465 Aftershocks halted by static stress shadows. *Nature Geoscience*,
466 5:doi:10.1038/ngeo1465, 410–413.

467 van der Elst, N. and Brodsky, E. (2010). Connecting near-field and
468 far-field earthquake triggering to dynamic strain. *J. Geophys. Res.*,
469 115:doi:10.1029/2009JB006681.

470 Velasco, A. A., Hernandez, S., Parsons, T., and Pankow, K. (2008). Global
471 ubiquity of dynamic earthquake triggering. *Nature Geoscience*, 1:375–379.

472 von Huene, R. and Scholl, D. W. (2012). Observations at convergent margins
473 concerning sediment subduction, subduction erosion, and the growth of
474 continental crust. *Rev. Geophys.*, 29:279–316.

475 Wells, D. L. and Coppersmith, K. J. (1994). New Empirical Relationships
476 among Magnitude, Rupture Length, Rupture Width, Rupture Area, and
477 Surface Displacement. *Bull. Seismol. Soc. Am.*, 84:974–1002.

478 Yue, H., Lay, T., and Koper, K. D. (2012). En Echelon and Orthogonal
479 Fault Ruptures of the 11 April 2012 Great Interplate Earthquake. *Nature*,
480 490:245–249.

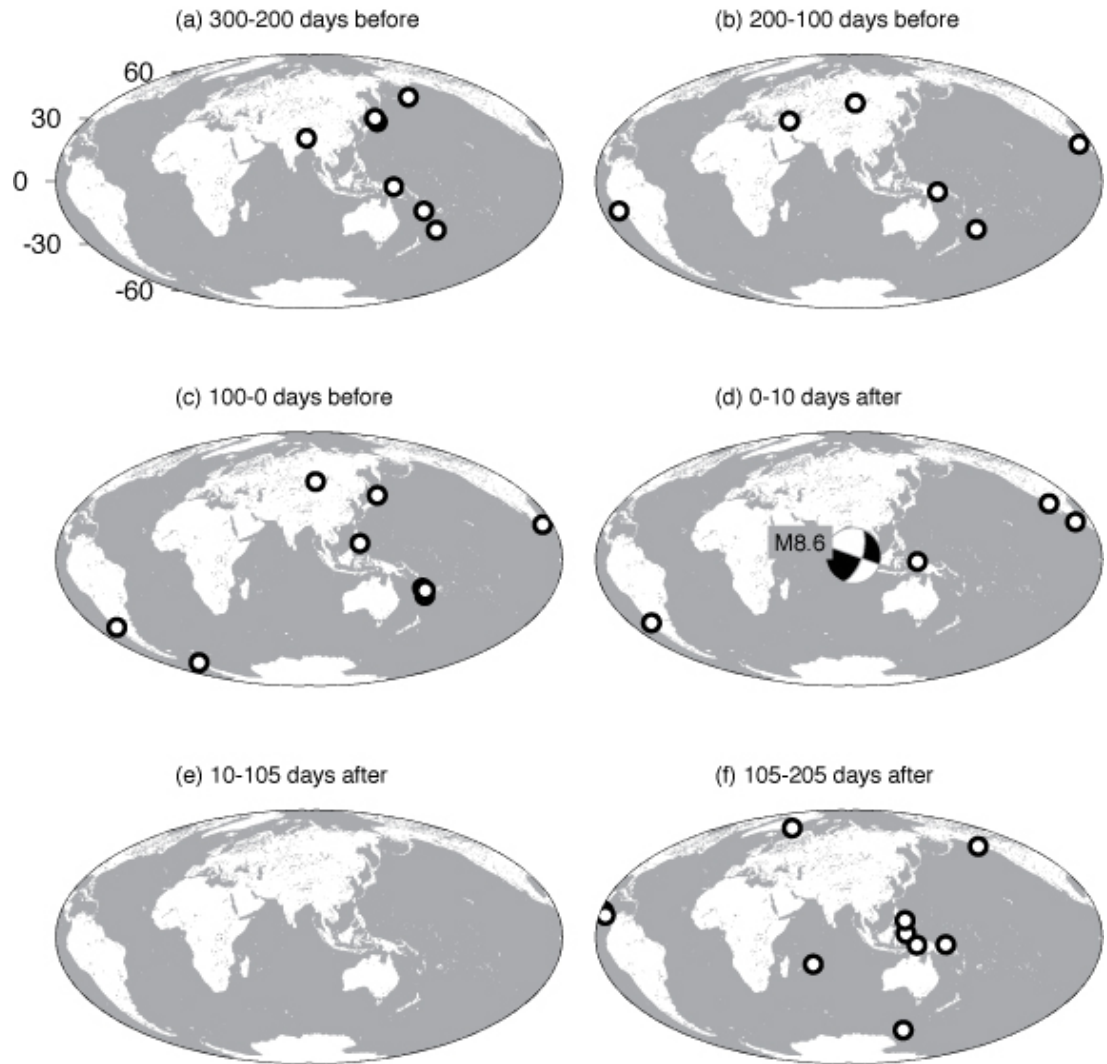


Figure 1: Remote global $M \geq 6.5$ seismicity (0-100 km depth here and in subsequent figures) over the indicated time periods. Time is relative to the origin time of the 11 April 2012 Indian Ocean event. Remote events are defined as those > 1500 km from the epicenter of the 11 April 2012 Indian Ocean event (indicated in (d)).

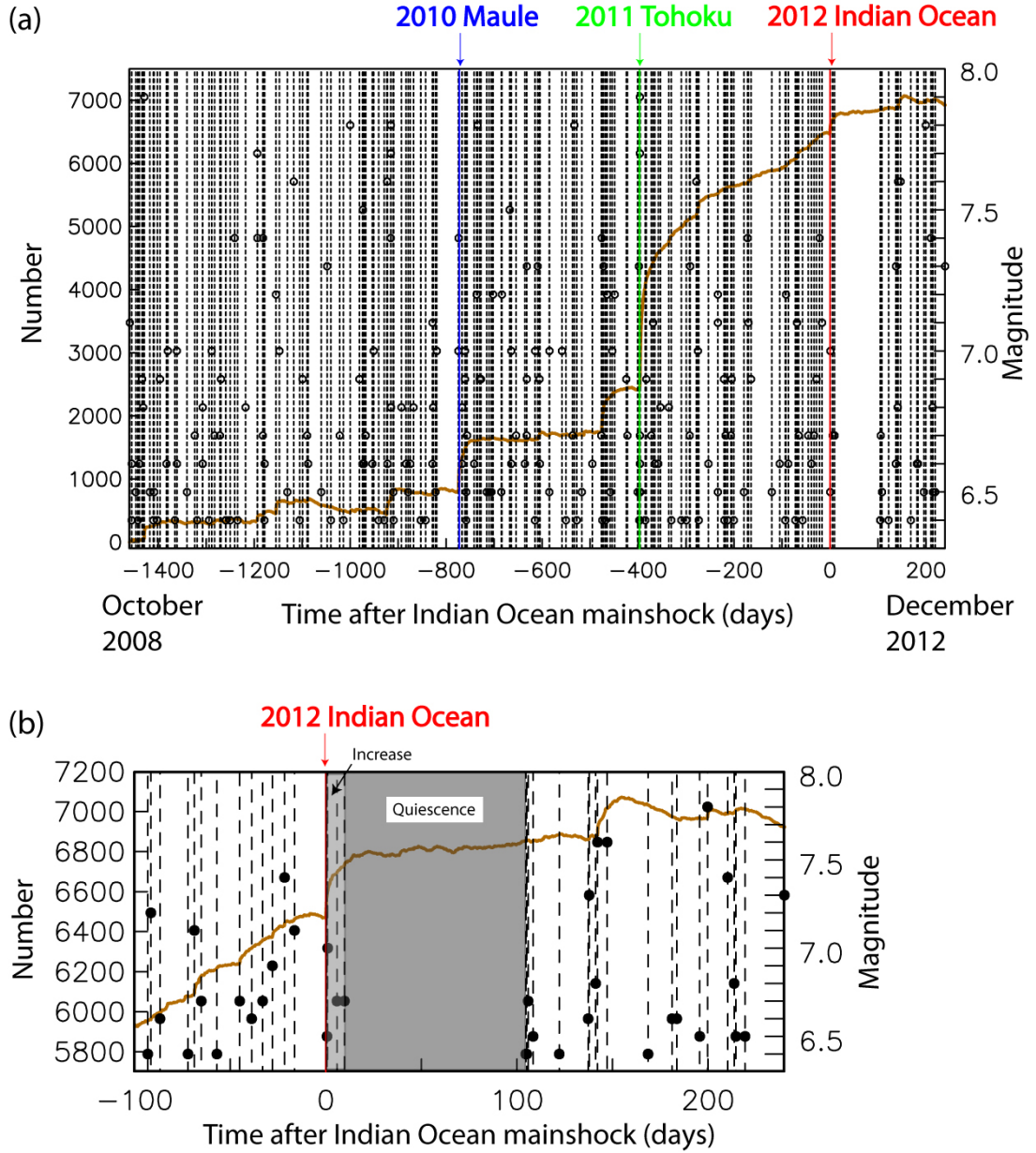


Figure 2: (a) Cumulative number of $M \geq 4.5$ earthquakes reduced by 13 events/day. Time is relative to the origin time of the 11 April 2012 Indian Ocean event. Vertical dashed lines indicate times of $M \geq 6.4$ events, with magnitudes given by corresponding open circles. Catalog is unedited (i.e. no 1500 km exclusion zones). (b) is a close-up of (a) over the period from 100 days before to 240 days after the mainshock.

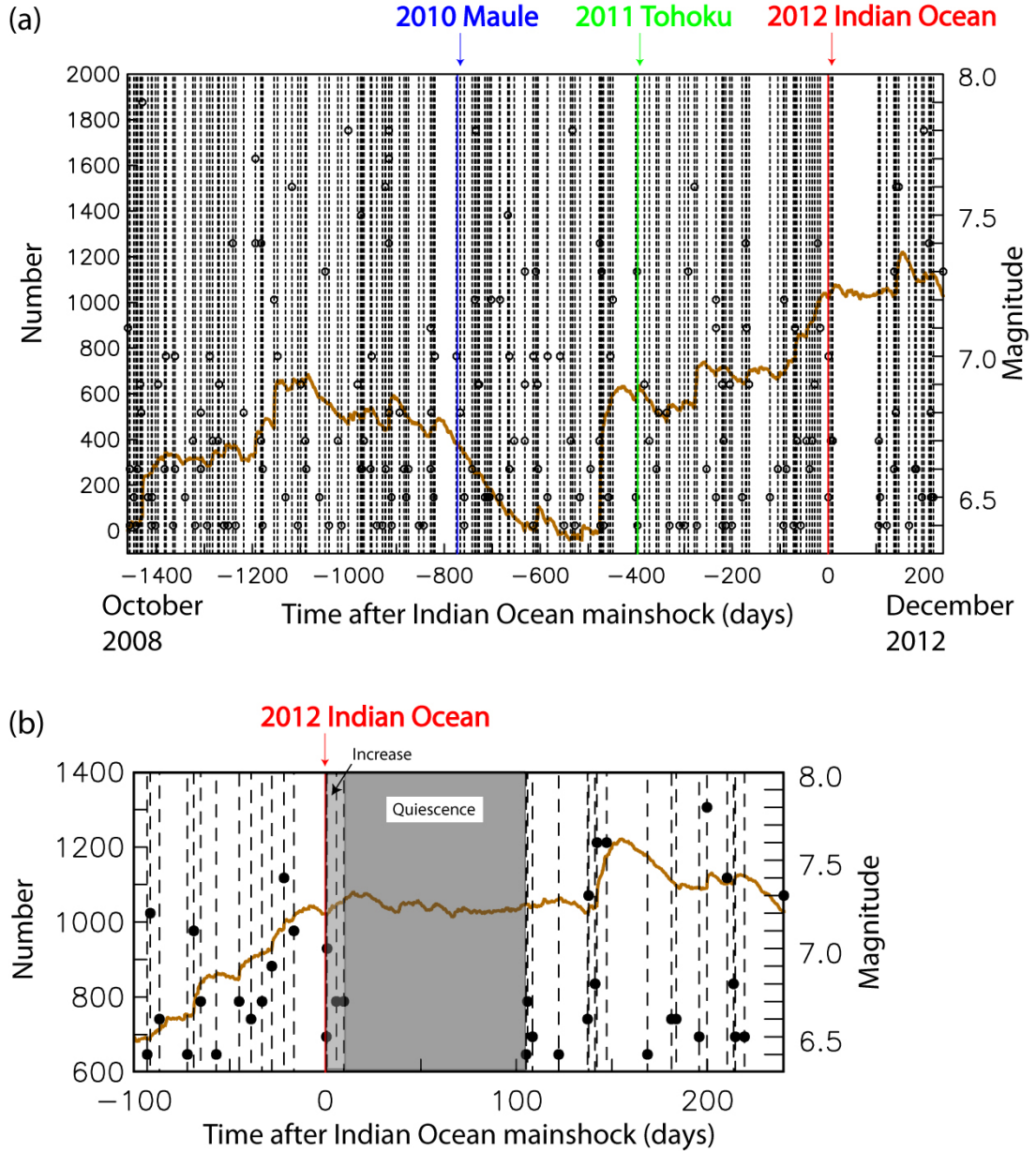


Figure 3: (a) Cumulative number of $M \geq 4.5$ earthquakes reduced by 13 events/day. Time is relative to the origin time of the 11 April 2012 Indian Ocean event. Vertical dashed lines indicate times of $M \geq 6.4$ events, with magnitudes given by corresponding open circles. Events are edited with large-mainshock declustering. (b) is a close-up of (a) over the period from 100 days before to 240 days after the mainshock.

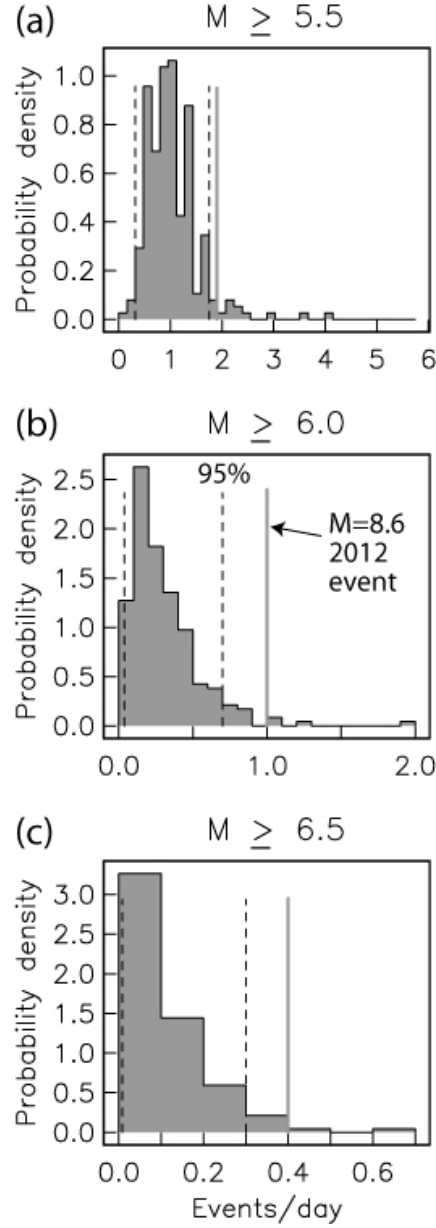


Figure 4: Empirical probability density functions of the remote seismicity rate above a given magnitude during the 10 days following a $M \geq 7$ mainshock. They are calculated using the sampling procedure described in the Methods section of Pollitz et al. (2012); 243 $M \geq 7$ mainshocks during the 20 years preceding the April 2012 Indian Ocean event are employed. All seismicity rates are ‘remote’ in the sense that events occurring after a given $M \geq 7$ mainshock are constrained to lie outside a spherical cap of radius 1500 km centered on that mainshock. Dashed lines indicate the 5% and 95% tails of the distributions, and the vertical gray line denotes the observed remote seismicity rate during the 10 days following the April 2012 event.

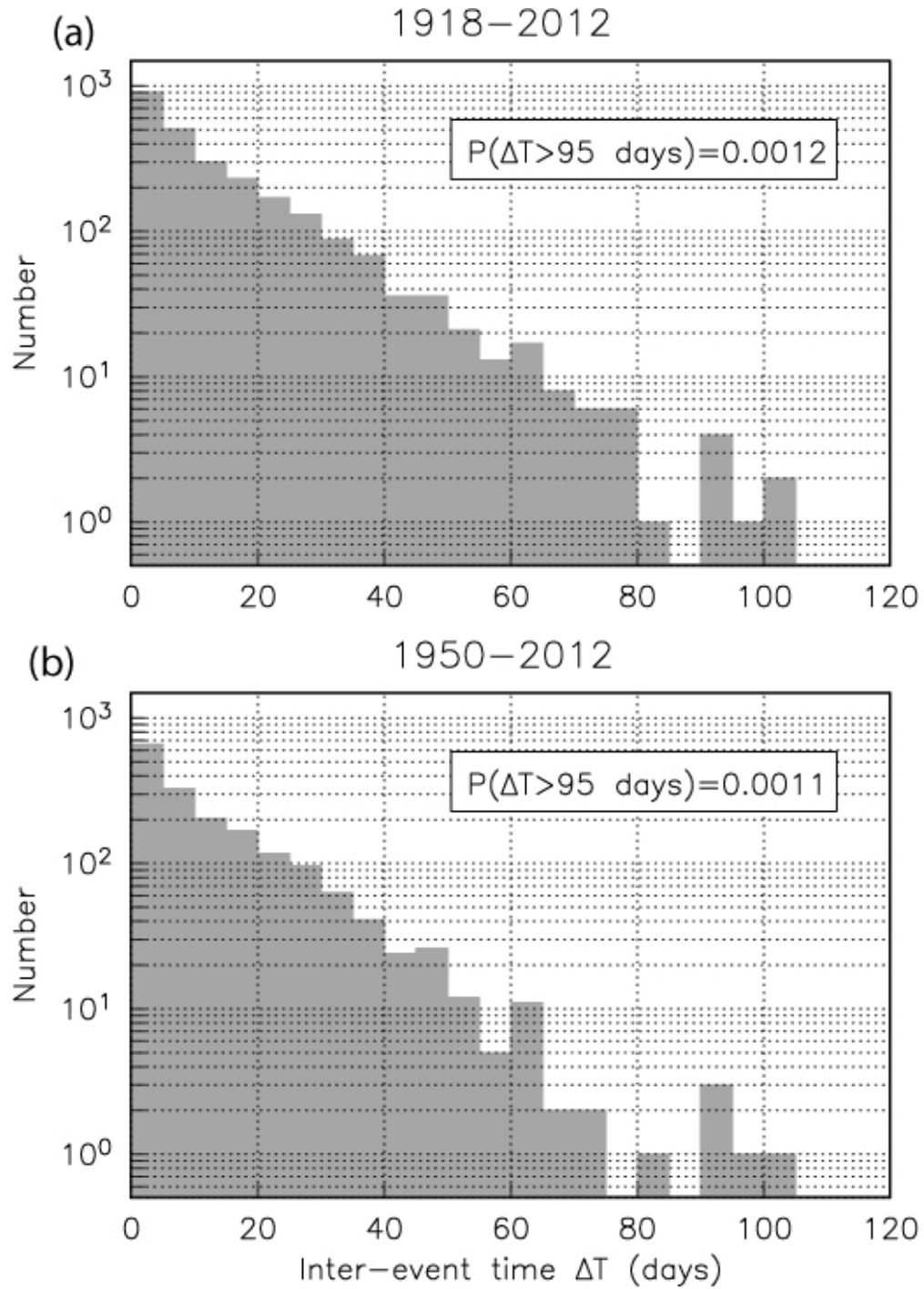


Figure 5: Histograms of global $M \geq 6.5$ inter-event times ΔT using the ISC-GEM catalog for the periods (a) 1918 to 11 April 2012 and (b) 1950 to 11 April 2012. Large-mainshock declustering is applied. Probability of ΔT exceeding 95 days is indicated in each case.

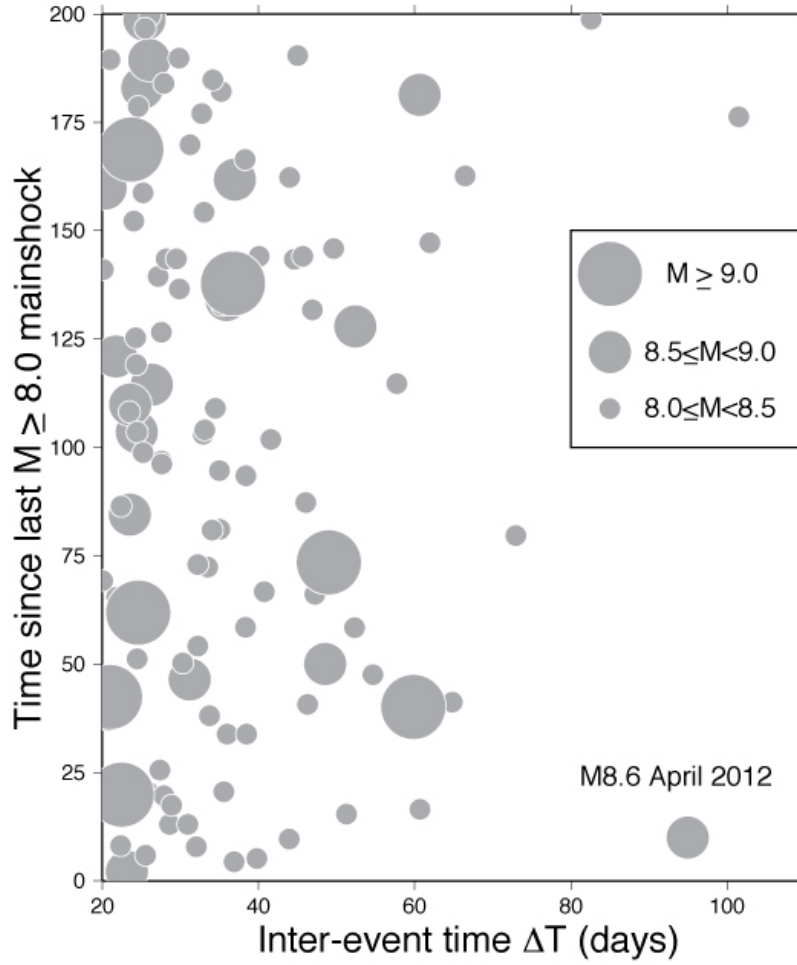


Figure 6: $M \geq 6.5$ inter-event time ΔT versus the time since the last $M \geq 8.0$ mainshock preceding the beginning of the time interval bracketing two consecutive $M \geq 6.5$ events. Events are extracted from the 1918 - July 2012 ISC-GEM catalog. Large-mainshock declustering is applied. Mainshocks may appear more than once because they may be associated with more than one pair of consecutive $M \geq 6.5$ events.

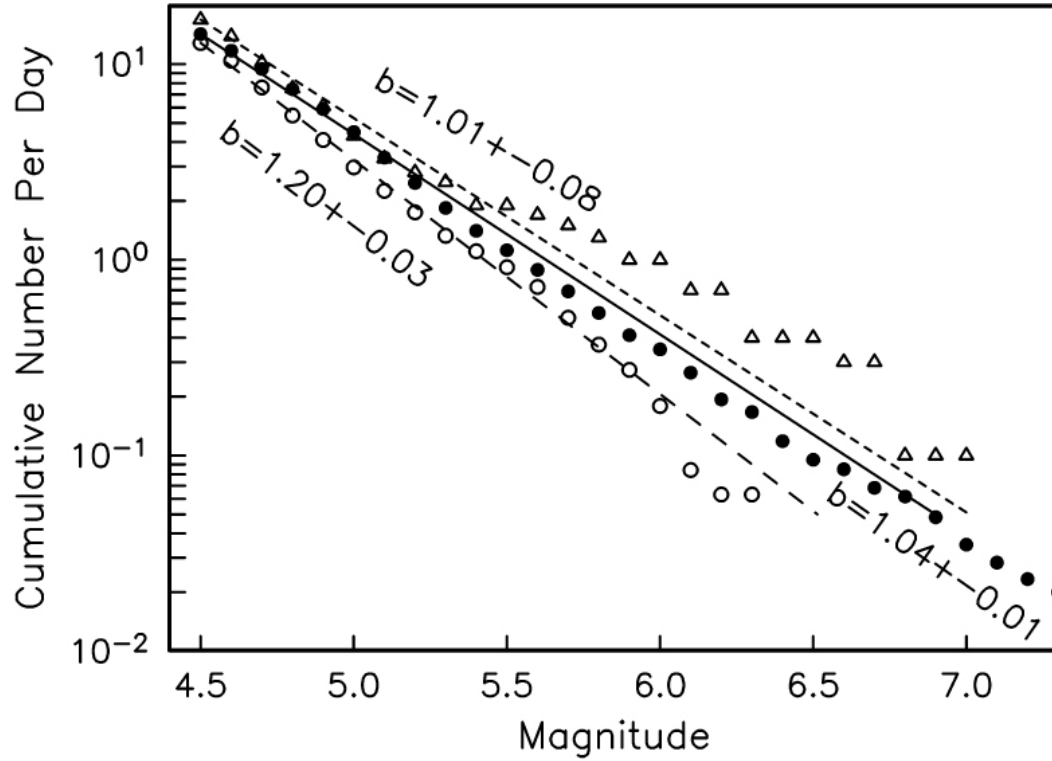


Figure 7: Cumulative number of ‘remote’ events as a function of magnitude, normalized to the time interval being considered. Filled circles represent background remote events. Triangles represent remote events during the period 0 to 10 days following the April 2012 mainshock. Open circles represent remote events during the period 10 to 105 days following the April 2012 mainshock. Lines indicate the corresponding fit to a linear magnitude-frequency relationship with b -values calculated using maximum likelihood estimation.

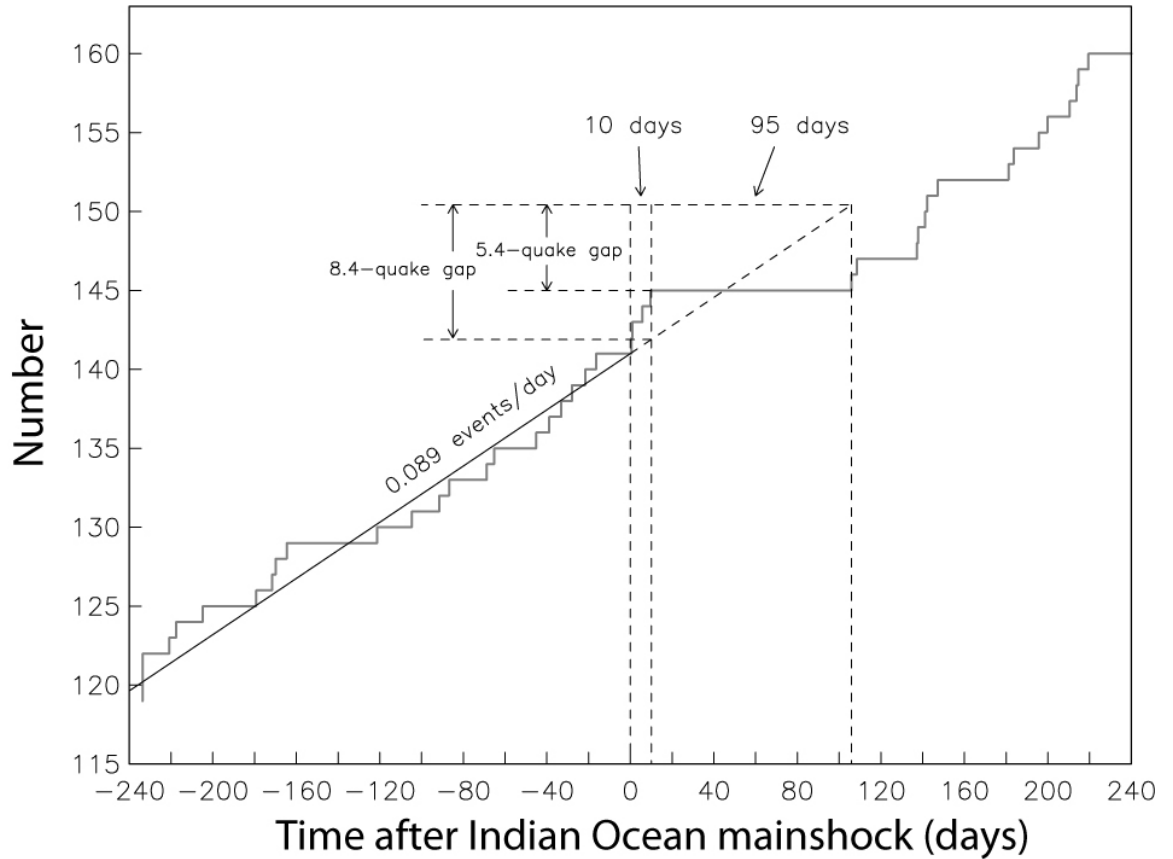


Figure 8: Cumulative number of $M \geq 6.5$ events from 240 days before to 240 days after the April 2012 Indian Ocean mainshock using the NEIC catalog with large-mainshock declustering. Although a 5.4-event gap apparently results when examining the budget of $M \geq 6.5$ events expected to occur within 105 days after the mainshock, the four events which occurred within the first 10 days – because they are dynamically triggered – contribute little to the budget of expected $M \geq 6.5$ quake productivity for this time period. This results in an effective 8.4-quake gap during the 95-day quiescent period. The background rate of 0.089 events/day is based on the 30-year catalog NEIC catalog and ISC-GEM catalog.